

ANALYSIS OF TROUGH FORMATION AND LATERAL STEERING OF A WEB DUE TO A TAPERED DOWNSTREAM ROLLER

by

J.A. Beisel and J.K. Good
Oklahoma State University
USA

ABSTRACT

Cylindrical rollers are never perfectly cylindrical. A common defect of a cylindrical roller is radial taper. A roller with a radial taper will induce a lateral shear force into the web. This shear force will cause a steering effect as well as a cross machine direction compressive stress which can lead to the formation of troughs and wrinkles in a web. This publication addresses these topics and presents a model to help determine the specification for taper in "cylindrical" rollers. An analytical model is presented, experiments were performed, and the data was compared to predictions from the proposed model.

NOMENCLATURE

a	span length
A	area of cross section of web
A_s	area of beam which reacts shear
b	web width
f_{yi}	lateral force at upstream roller
f_{yj}	lateral force at downstream roller
E	Young's Modulus
G	shear modulus
h	web thickness
I	web area moment of Inertia
k	shape factor for shear stress distribution
m	slope of radial profile of tapered roller
m_{cr}	critical slope of tapered roller needed to induce troughs in the web
M_i	bending moment in web at upstream roller
M_j	bending moment in web at downstream roller
r	radius
R_o	nominal roller radius

T	web line tension
v_i	lateral deflection of web at upstream roller
v_j	lateral deflection of web at downstream roller
V	web velocity
V_{avg}	average web velocity
x	coordinate that aligns with the MD direction
y	coordinate that aligns with the CMD direction
ϵ_{md}	machine direction strain
γ_{xy}	shear strain
ν	Poisson's Ratio
ϕ	shear parameter
σ	stress
σ_{md}	stress in the machine direction
σ_x	stress in the x direction
σ_y	stress in the y direction
σ_{yer}	stress needed to induce troughs in the web
θ_i	end rotation of the web at the upstream roller
θ_j	end rotation of the web at the downstream roller
τ_{max}	maximum shear stress
τ_{cr}	shear stress needed to induce troughs in the web
ω	angular velocity of the roller

INTRODUCTION

The most common means of supporting and transporting webs in web handling processes is via rollers. Web roller interaction (with the exception of web guides) is typically not intended to induce lateral forces into the web. However, there are many circumstances that do in fact introduce these lateral forces into webs, such as misaligned rollers, cambered webs, and rollers with a non-cylindrical profile. Out of all the defects a machined roller could possess, a uniform taper is likely to be the most common. A tapered roller could be created inadvertently by a misaligned tailstock, a lathe with worn ways, or flexure of material and clamping apparatus.

The problem of a web traveling over a tapered roller has been discussed by Swift [8] and Shelton [6], [7]. Swift proposes limitations for how much taper is needed on a roll to correct for drives that maybe misaligned, twisted, or offset, as well as for the case of a cambered belt. Shelton analyses the case of a downstream tapered roller in an isolated span. He proposed a classical theory for deflection with consideration of web line tension [6]. He later presented a model for deflection but with the inclusion of shear effects [7]. He additionally developed a model to predict instability in the web. One goal of this effort is to provide experimental data for comparison to theory.

This paper presents yet another approach to classical analysis by treating the isolated web span as a beam and employing a stiffness matrix approach to determine the deflection of the web. Web instability is analyzed by using the Timoshenko [9] instability criteria for a plate loaded with and across its length.

Experiments were conducted for both deflection and web buckling, which will be defined here as formation of out of plane troughs in the web. The results are presented for comparison to the presented models as well as a discussion of the associated boundary conditions of the web.

WEB DEFLECTION

In the analysis of a web passing over a tapered roller, an assumption will be made that the web will traverse the roller at the same speed as the roller surface in that region. A high web to roller coefficient of friction will be assumed and as a result it will be further assumed that the web span studied is isolated and free of moment transfer from or onto preceding spans. Moment transfer is the condition where web to roller traction is insufficient to isolate a span from bending moments and shear forces in adjacent spans. The result is a bending moment in one span can traverse across a roller and affect another web span. Further information on moment transfer can be found in [1]. Analysis will be based on classical beam theory incorporating shear and tension effects using a stiffness matrix approach.

Boundary Conditions

A rotating tapered roller has a surface velocity profile across its width that varies proportionately with its linearly varying radius. With sufficient friction the web will conform to this velocity profile and thus one side of the web must travel faster over a further distance than the other side of the web. This difference in velocity results in an applied moment across the width of the web. This moment will be calculated in the next development.

The radius of the roller is given by equation (1) where R_o is the nominal diameter at the center, m is the slope of the radial taper (cm/cm), and y is the CMD position across the roller with its origin at the center.

$$r(y) = m \cdot y + R_o \quad \{1\}$$

The local and average velocities of the web are given by equation (2) in which ω represents the angular velocity of the roller and V is the tangential velocity of the web.

$$V(y) = r(y) \cdot \omega = (m \cdot y + R_o) \cdot \omega \quad \text{and} \quad V_{avg} = R_o \cdot \omega \quad \{2\}$$

The difference in velocity across the width of the web causes a similarly varying difference in strain and hence stress. The strain profile created by the tapered roll is expressed in equation (3). It should be noted that equation (3) does not account for the additional strain and stress due to web line tension.

$$\epsilon_{md}(y) = \frac{V(y) - V_{avg}}{V_{avg}} = \frac{m \cdot y}{R_o} \quad \text{and} \quad \sigma(y) = E \cdot \epsilon_{md}(y) = \frac{E \cdot m \cdot y}{R_o} \quad \{3\}$$

Integrating the varying stress across the width of the web yields the moment induced by the tapered roller. A minus sign appears based on the definitions of positive moments (Figure 1), and roller slope.

$$M_j = \int_{-b/2}^{b/2} -\sigma(y) \cdot h \cdot y \cdot dy = \int_{-b/2}^{b/2} \frac{-E \cdot m \cdot h \cdot y^2}{R_o} \cdot dy = \frac{-m \cdot E \cdot h \cdot b^3}{12 \cdot R_o} \quad \{4\}$$

The variables in equation (4) represent: h = web thickness, b = web width, E = Young's

Modulus, and M_j being equal to the moment applied at the down stream roller.

The other boundary conditions are the upstream deflection and the end rotations which are related to the slope of the beam at the ends. The upstream deflection (v_i) is arbitrary when considering the influence of a tapered roller at the downstream end of the span on change in lateral deformation and force in a web span. Since it is arbitrary it will be set to zero. The rotation of the cross section at the beam ends is given by equation (5) for a Timoshenko beam [5].

$$\theta_{i,j} = \frac{dy}{dx} + \gamma_{xy} = -\frac{f_{yi}}{G \cdot A_s} \quad \{5\}$$

The condition of normal entry or exit for a web approaching or exiting a roller requires the slope of the lateral deformation $(dv/dx)_{i,j}$ to be zero in expression (5). Equation (5) sets identical boundary conditions for the rotation of the cross section at the upstream and downstream end of the web span. In Euler beam theory, shear strains are not considered, the rotation of the cross section ($\theta_{i,j}$) and the beam slope become one and the same per expression (5). Euler theory is reserved for cases in which bending stresses and strains are predominate ($a/b > 10$). Timoshenko beam theory is applicable for both cases where shear and strain is appreciable and where it is not, therefore will be used herein.

Beam Model

The web is modeled as a typical beam with the deformations being represented by a stiffness matrix. Przemieniecki [4] and others have demonstrated the use of stiffness matrixes to relate forces and deformations to beam elements. One such matrix was constructed by starting with a simple beam matrix, adding terms to account for the effects of shear, and finally superimposing this matrix with a matrix that represents the stiffness of the web due to web line tension. The resulting stiffness matrix is shown in equation (6).

$$\begin{pmatrix} f_{yi} \\ M_i \\ f_{yj} \\ M_j \end{pmatrix} = \begin{bmatrix} \frac{12 \cdot E \cdot I}{a^3 \cdot (1 + \phi)} + \frac{6 \cdot T}{5 \cdot a} & \frac{6 \cdot E \cdot I}{a^2 \cdot (1 + \phi)} + \frac{T}{10} & \frac{-12 \cdot E \cdot I}{a^3 \cdot (1 + \phi)} - \frac{6 \cdot T}{5 \cdot a} & \frac{6 \cdot E \cdot I}{a^2 \cdot (1 + \phi)} + \frac{T}{10} \\ \frac{6 \cdot E \cdot I}{a^2 \cdot (1 + \phi)} + \frac{T}{10} & \frac{E \cdot I \cdot (4 + \phi)}{a \cdot (1 + \phi)} + \frac{2 \cdot T \cdot a}{15} & \frac{-6 \cdot E \cdot I}{a^2 \cdot (1 + \phi)} - \frac{T}{10} & \frac{E \cdot I \cdot (2 - \phi)}{a \cdot (1 + \phi)} - \frac{T \cdot a}{30} \\ \frac{-12 \cdot E \cdot I}{a^3 \cdot (1 + \phi)} - \frac{6 \cdot T}{5 \cdot a} & \frac{-6 \cdot E \cdot I}{a^2 \cdot (1 + \phi)} - \frac{T}{10} & \frac{12 \cdot E \cdot I}{a^3 \cdot (1 + \phi)} + \frac{6 \cdot T}{5 \cdot a} & \frac{-6 \cdot E \cdot I}{a^2 \cdot (1 + \phi)} - \frac{T}{10} \\ \frac{6 \cdot E \cdot I}{a^2 \cdot (1 + \phi)} + \frac{T}{10} & \frac{E \cdot I \cdot (2 - \phi)}{a \cdot (1 + \phi)} - \frac{T \cdot a}{30} & \frac{-6 \cdot E \cdot I}{a^2 \cdot (1 + \phi)} - \frac{T}{10} & \frac{E \cdot I \cdot (4 + \phi)}{a \cdot (1 + \phi)} + \frac{2 \cdot T \cdot a}{15} \end{bmatrix} \begin{pmatrix} v_i \\ \theta_i \\ v_j \\ \theta_j \end{pmatrix} \quad \{6\}$$

The previous stiffness matrix carries the following sign conventions and definitions.

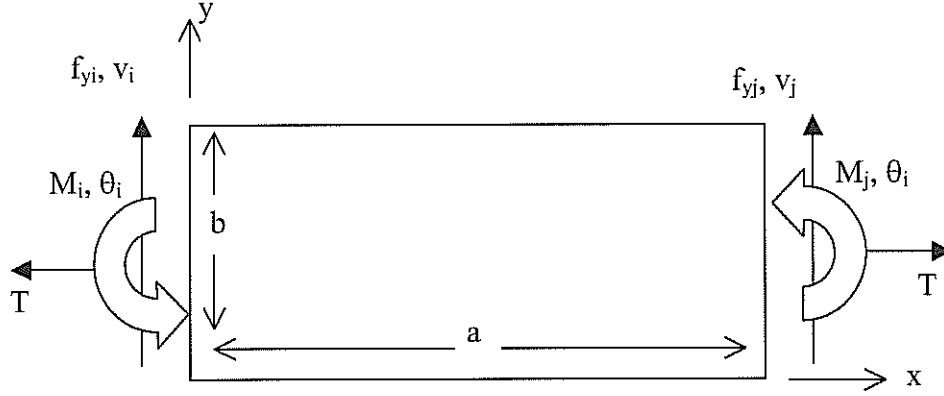


Figure 1 - Positive Sign Conventions of Beam

In addition, ϕ represents a shear term and is defined by equation {7}.

$$\phi = \frac{12 \cdot E \cdot I}{G \cdot A_s \cdot a^2} \quad \{7\}$$

In equation (7), E_x is Young's Modulus in the machine direction (x axis), I is the moment of inertia of a cross section given by $I = (h \cdot b^3)/12$, and A_s is the area of the beam cross section reacting shear which for a rectangular cross section has been shown to equal $5/6 b \cdot h$ [10].

After applying the previously discussed boundary conditions and expanding the 3rd and 4th rows of equation (6), solving them for the downstream shear force (f_{yj}), and setting them equal to each other, the resulting expression can be solved for the downstream deflection v_j . This result is given in equation (8) after the substitution of the applied moment at the tapered roller.

$$v_j = \frac{m \cdot h \cdot b^3 \cdot E}{6 \cdot R_o} \cdot \frac{-60 \cdot E \cdot I + (5 \cdot G \cdot A_s \cdot a^2 - T \cdot a^2) \cdot (1 + \phi)}{[60 \cdot E \cdot I + T \cdot a^2 \cdot (1 + \phi)] \cdot (T + G \cdot A_s)} \quad \{8\}$$

In a similar manner the shear force present at the downstream roller may be found by eliminating v_j and solving for f_{yj} . The result yields equation (9).

$$f_{yj} = \frac{m \cdot h \cdot b^3 \cdot E}{R_o \cdot a} \cdot \frac{G \cdot A_s \cdot [10 \cdot E \cdot I + T \cdot a^2 \cdot (1 + \phi)]}{[60 \cdot E \cdot I + T \cdot a^2 \cdot (1 + \phi)] \cdot (T + G \cdot A_s)} \quad \{9\}$$

WEB INSTABILITY

A relevant instability criteria was developed by Good [2] that builds on Timoshenko's model of a plate loaded in plane along both axis [9] combined with orthotropic web properties as proposed by Lekhnitskii [3]. The relevant result, equation (10), is an expression that lists the critical cross machine direction compressive stress for a coupon loaded in tension in the machine direction.

$$\sigma_{ycr} = \frac{-\pi \cdot h}{a} \cdot \sqrt{\frac{\sigma_{md} \cdot E}{3 \cdot (1-\nu^2)}} \quad \{10\}$$

The source of this compressive cross machine direction stress must be determined. The combination of a machine direction tensile stress and a cross machine direction shear stress will yield a compressive second principal stress. This stress is represented by equation (11).

$$\sigma_2 = \frac{\sigma_{md}}{2} - \sqrt{\left(\frac{\sigma_{md}}{2}\right)^2 + \tau^2} \quad \{11\}$$

It will be assumed this principal stress cannot be less than the stress at buckling given in expression (10). After substituting this limit for the principal stress, the critical value of the shear stress which is required to buckle the web can be calculated from equation (12).

$$\tau_{cr} = \sqrt{\left(\frac{\pi \cdot h}{a}\right)^2 \cdot \frac{\sigma_{md} \cdot E}{3 \cdot (1-\nu^2)} + \frac{\pi \cdot h}{a} \cdot \sqrt{\frac{\sigma_{md}^3 \cdot E}{3 \cdot (1-\nu^2)}}} \quad \{12\}$$

Shear stresses exist within the web as a result of the steering forces due to the tapered roller, equation (9). The shearing stress has a parabolic variation with respect to the y coordinate. Due to surface equilibrium it must dissipate to zero at the boundaries where $y = 0$ and $y = b$ as shown in Figure 1. The shear stress is at a maximum at the web center ($y = b/2$) where from strength of materials the value is known to be:

$$\tau_{max} = \frac{3}{2} \cdot \frac{f_{yj}}{b \cdot h} \quad \{13\}$$

If equation (9) is substituted into (13) the result can be solved for a critical radial taper that will induce troughs into a web span. This final result is given in equation (14).

$$m_{cr} = \frac{2 \cdot a \cdot R_o}{3 \cdot b^2 \cdot E} \frac{[60 \cdot E \cdot I + T \cdot a^2(1+\phi)](T + G \cdot A_s)}{G \cdot A_s [10 \cdot E \cdot I + T \cdot a^2(1+\phi)]} \sqrt{\left(\frac{\pi}{a}\right)^2 \frac{h \cdot T \cdot E}{b \cdot 3(1-\nu^2)} + \frac{\pi}{a} \sqrt{\frac{T^3 \cdot E}{b^3 \cdot h \cdot 3(1-\nu^2)}}} \quad \{14\}$$

Equation (14) gives us a model to predict the onset of troughs in a web span in terms of tension, web span, roller geometry, and web properties.

EXPERIMENTAL PROCEDURES

Creating Tapered Rollers

The first step in experimentation was the creation of tapered rollers. A roller with a variable taper, while desirable, would be difficult to produce. Since web line tension can easily be adjusted and has an impact on web stability, it was used as the test variable. A set of four tapered rollers were machined for the tests. The rollers were machined on a conventional lathe. The magnitude of the tapers were too small for use of conventional taper cutting techniques, so the tail stock was misaligned from the chuck to hold the work piece at an angle to the path of the tool post. This technique is acceptable for cutting small tapers but if the angle is too large, binding and slippage between the work piece and the chuck will occur. It should be noted that the work piece was held semi-cantilevered at the chuck and pinned at the tail stock.

The next step was to measure the taper or slope of the new rollers. This was done by mounting two laser micrometers on the tool post of a lathe. The roller could then be held by its shaft in the chuck and the micrometers moved along the roller axis measuring the diameter. The axial position was sensed using a potentiometer and a computer based data acquisition system recorded both measurements simultaneously. The setup is shown in Figure 2.

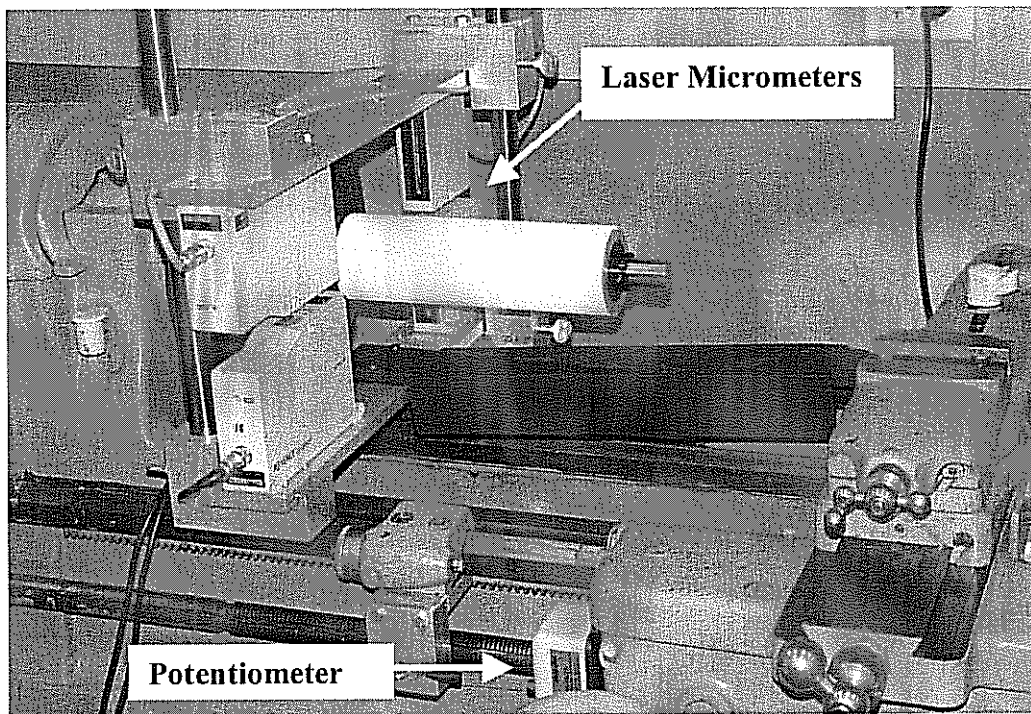


Figure 2 - Roller Profile Measurement

A sample of the output from the roll profiling system is displayed below in Figure 3.

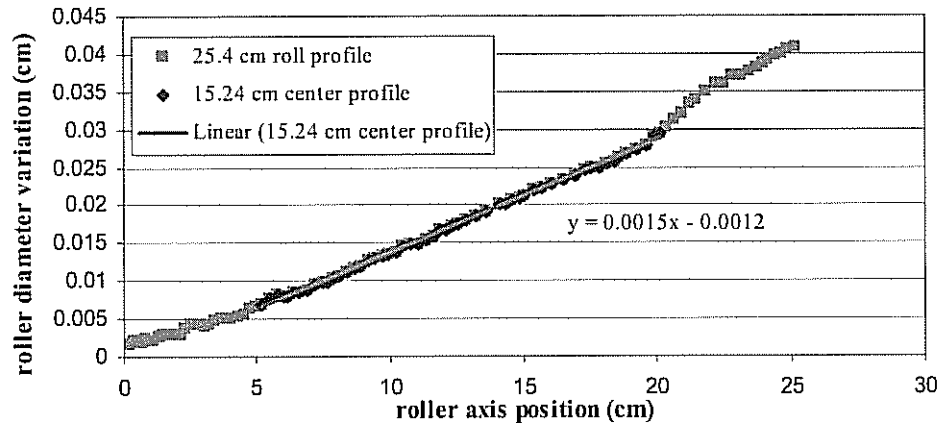


Figure 3 - Typical Roll Profile (roller is nominally 7.62 cm diameter)

The above figure displays the relative diametral profile of the roller with a reported slope of 0.00075 cm/cm of radial taper. The first trace is of the entire length of the roller, it should be noted that the data doesn't represent a perfect line and that attributing a slope to it can only be done on an average basis. The second trace represents the central portion of the roller where the web is assumed to contact ($b = 15.24$ cm in all tests). This portion is fit to a line and the slope of the line is reported as the diametral slope of the roller. It is important to note that the slope of the center portion is different than the average slope of the whole roller, and since the roller isn't perfect, web tracking position is important.

This procedure was repeated for to each roller five times during which each roller was rotated by a random amount. The resulting radial tapers for the rollers were: 0.00028, 0.00056, 0.00066, and 0.00075 cm/cm with standard deviations (for 5 tests) of: 1.3E-5, 5.7E-6, 5.4E-6, and 6.6E-6 respectively. A sample of measurements for the central portion of the rollers is displayed in Figure 4.

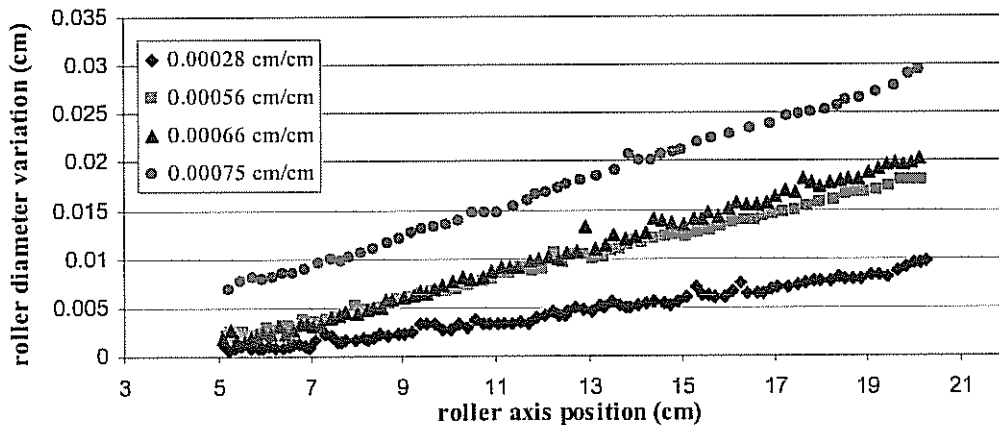


Figure 4 - Sample Roller Profiles (rollers are nominally 7.62 cm diameter)

Experimental Setup

Once the rollers were produced and their tapers were qualified, testing of deflection and trough formation could begin. The experimental setup utilized an unwind - rewind stand coupled with a test stand. The test stand was equipped with: a web guide to insure consistent entry into the test span, load cells located near to the test span to ensure accurate knowledge of the web line tension, high friction tape on the entry span roller to limit moment transfer into the test span from upstream and on the downstream roller to limit slippage, and multiple downstream roller positions for testing of various web span lengths. The setup is shown in Figure 5.

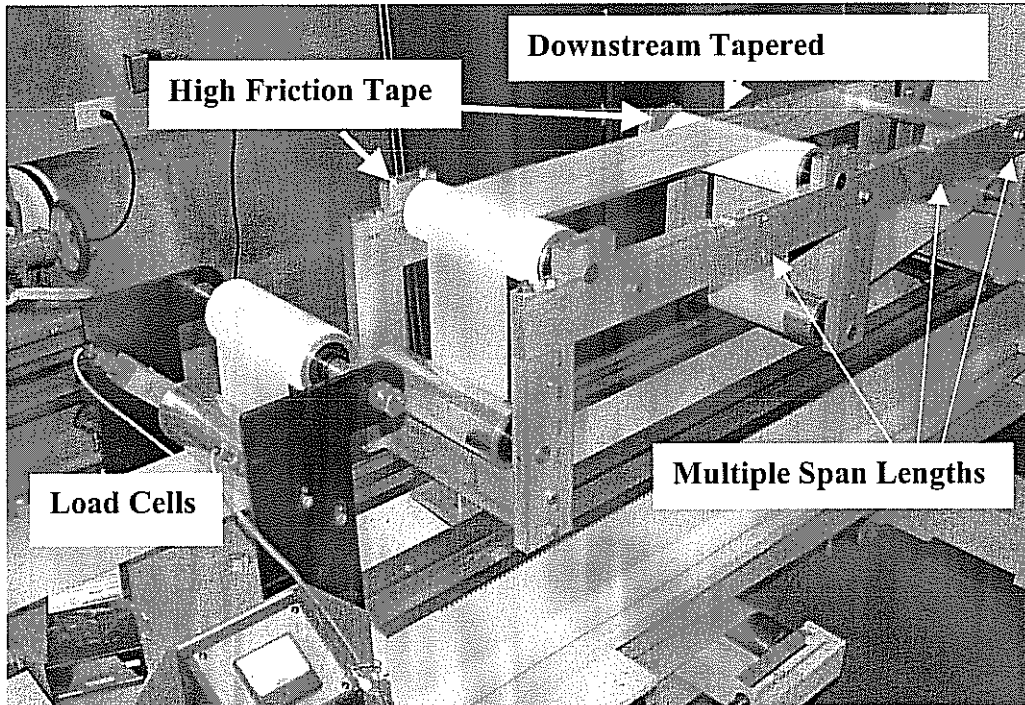


Figure 5 - Taper Roller Test Stand

Deflection Data

The data for the deflection of a web due to a tapered roller was measured by mounting a laser micrometer immediately before the upstream roller in our test span. A similarly mounted laser micrometer was mounted immediately downstream from the web span in question. The web line was then brought to speed and tension and the position of the web at both ends of the span were recorded through averaging by a data acquisition system. The web line was then stopped, the tapered roller flipped over to steer the web in the opposite direction, and the web line was again brought up to speed and tension. The positions of the web were again recorded. This was done so the effects of web camber, if present, could be eliminated from the result. The values reported for deflection were an average of the right and left deflection measurements. The configuration of the micrometers can be seen below in Figure 6.

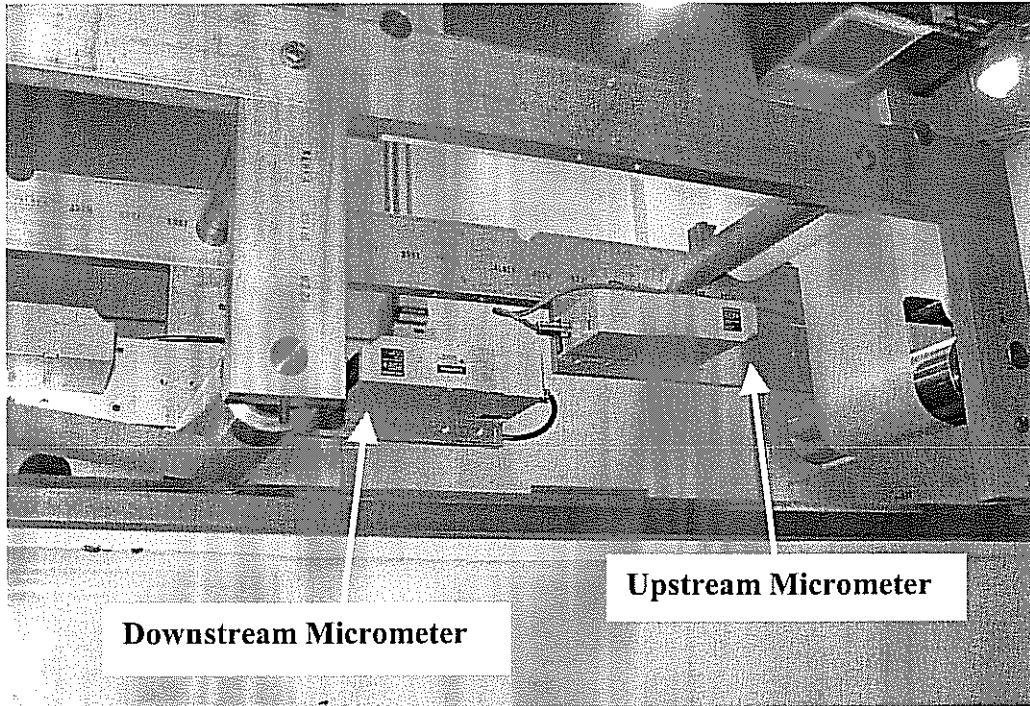


Figure 6 – Deflection Measurement

The first material tested was an opaque polyester. The fact that this material was not transparent was essential for use with the laser micrometers. The MD Young's modulus of the web was tested and found to be 4.9 GPa. The polyester web was assumed to be isotropic and homogeneous. All webs tested throughout this paper were 15.24 cm wide.

The plots presented in Figures 7 – 11 show a comparison of the beam model presented in equation (8) to experimental data. Each plot shows 3 span lengths and indicates whether the web was planar or if troughs were present when the measurement was taken. This distinction between the web being planar or "troughed" is based on later data presented in Figures 13 – 16 instead of actual observations since some of the data points may have been near the transition point and thus may have been difficult to accurately determine.

It should be noted that the deflection of the web is seemingly unaltered by the presence of troughs in the web span. Results from five different web line tensions are presented but it can be seen by comparing the scales on the different plots that the effect of tension is quite small in the case of deflection due to a tapered roller, at least under the range of span and web parameters tested here.

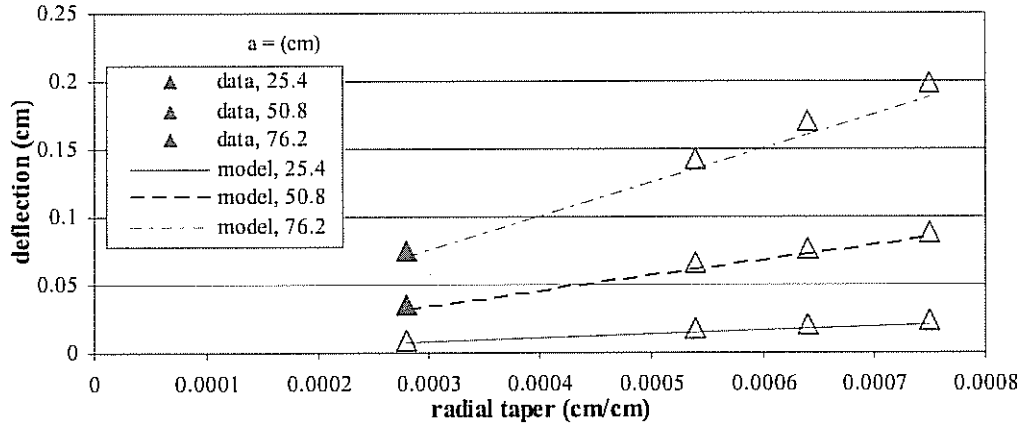


Figure 7 – 23.4 μm Polyester, $T = 44.5$ N (open triangles indicate troughs in web)

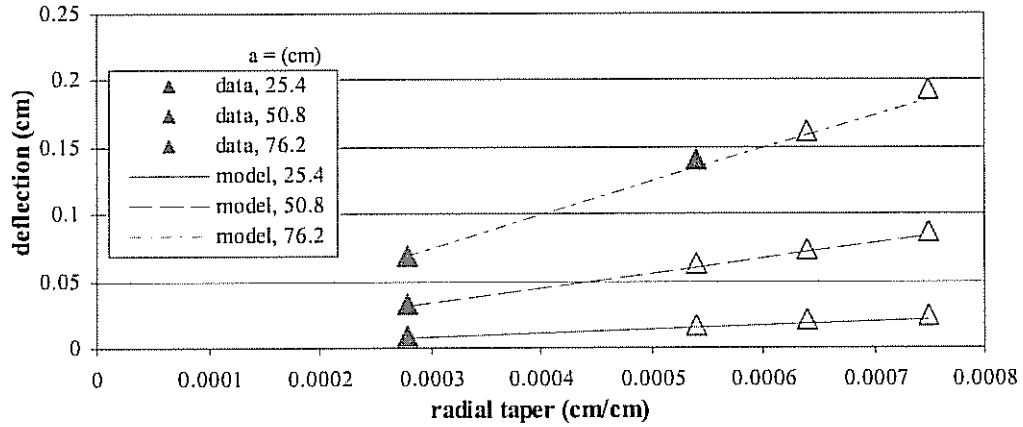


Figure 8 – 23.4 μm Polyester, $T = 66.7$ N (open triangles indicate troughs in web)

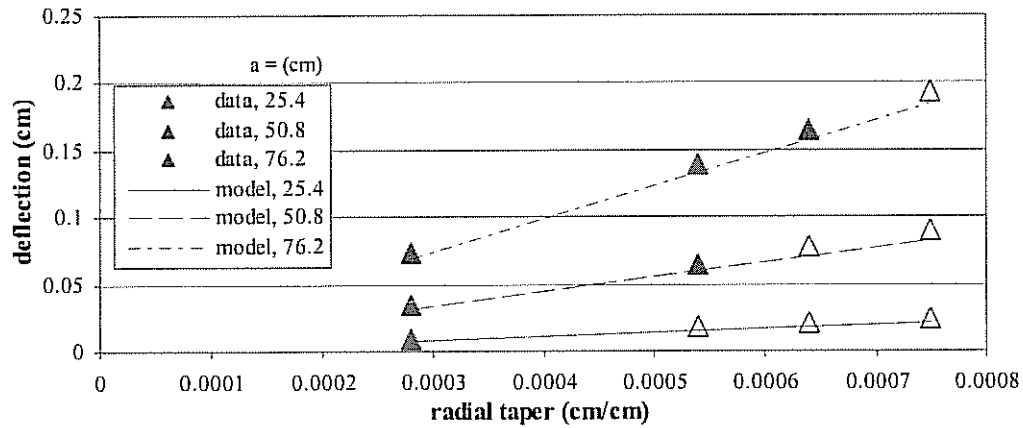


Figure 9 – 23.4 μm Polyester, $T = 89.0$ N (open triangles indicate troughs in web)

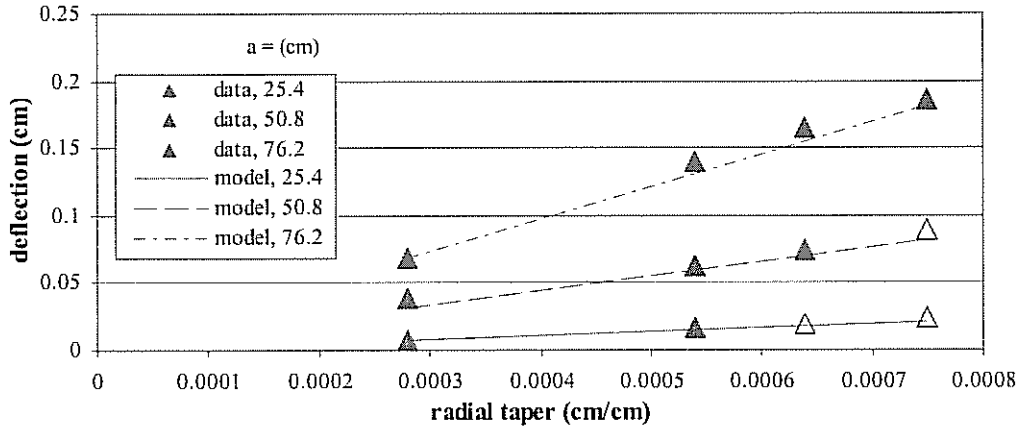


Figure 10 – 23.4 μm Polyester, $T = 111.2 \text{ N}$ (open triangles indicate troughs in web)

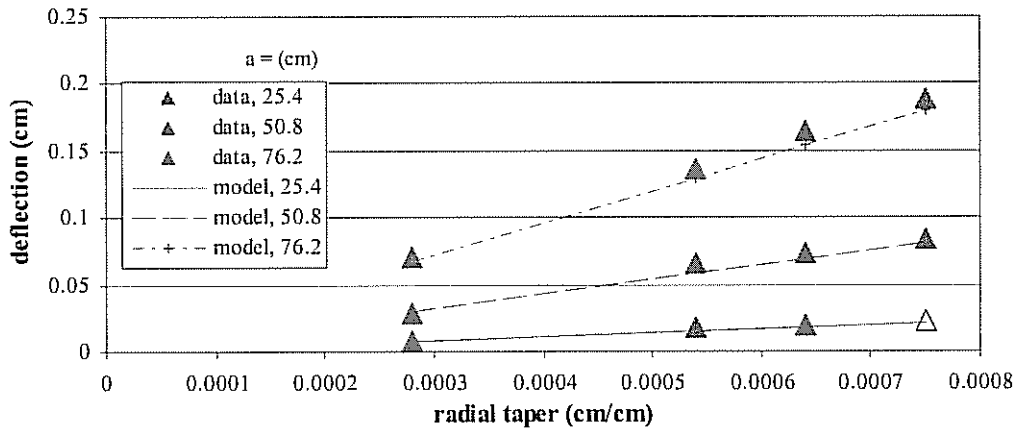


Figure 11- 23.4 μm Polyester, $T = 133.4 \text{ N}$ (open triangles indicate troughs in web)

Trough Formation Data

The same web used in the web deflection measurements was used in determining the onset of trough formation in a web span due to a tapered roller. Measurements were taken visually. This was accomplished with the assistance of a plane of laser light intersecting the web span at a low angle in incidence. The result is a straight line across the web span when the web is planar and a wavy curve that moves with the troughs when they are present, this can be seen clearly in Figure 12. Unlike the results of web deflection, the effect of web line tension on web stability is substantial. The determination of the onset of trough formation was accomplished by increasing web line tension until the wavy laser line went straight indicating a planar web and then tension was decreased to make sure the troughs immediately reformed. This was done again with the roller flipped over and the results of a right vs. left trough measurement were averaged. Every data point presented was the result of an average of three tests. Figures 13 – 16 depict 4 different web spans tested over the range of rollers available.

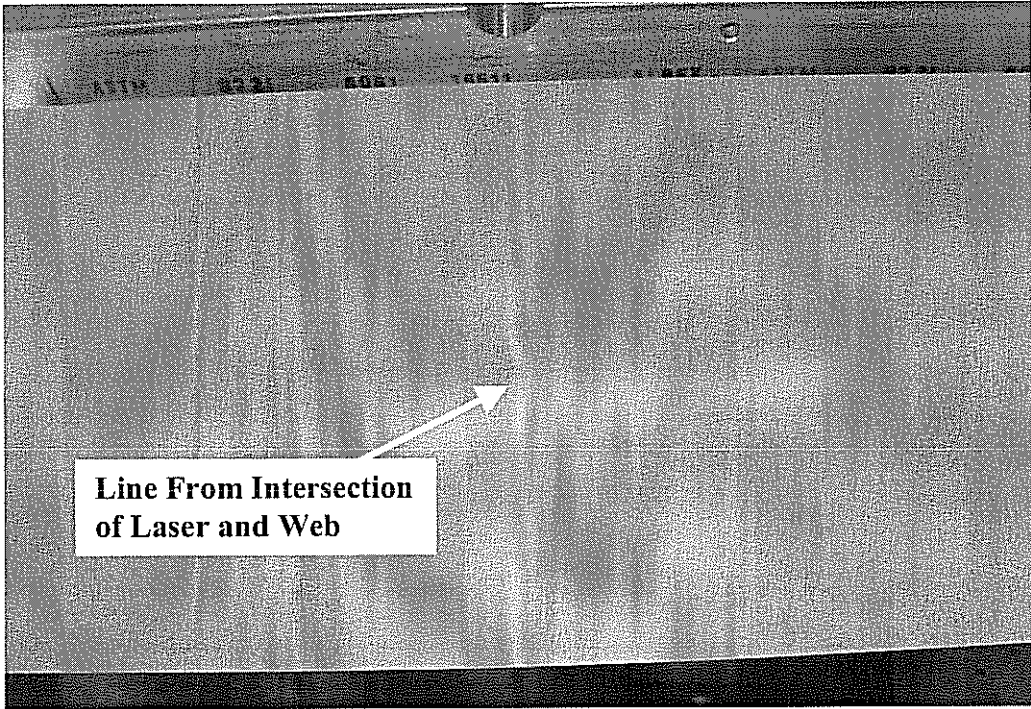


Figure 12 – Trough Visualization

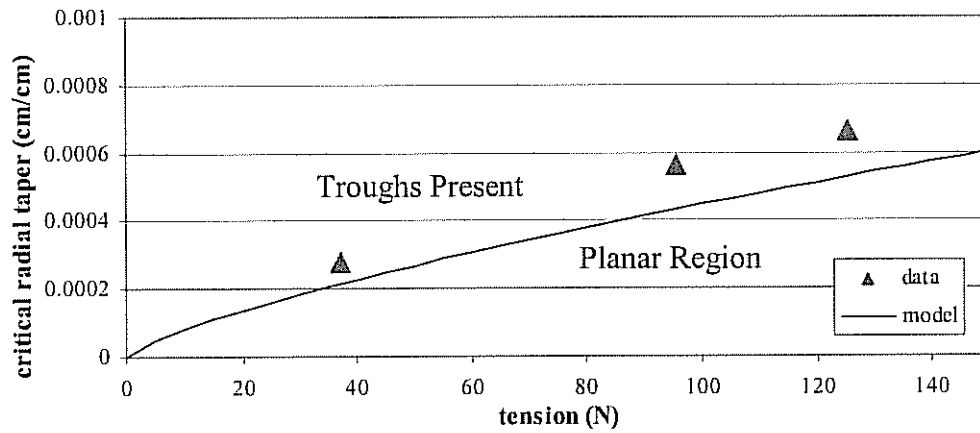


Figure 13 – 23.4 μm Polyester, $a = 25.4$ cm

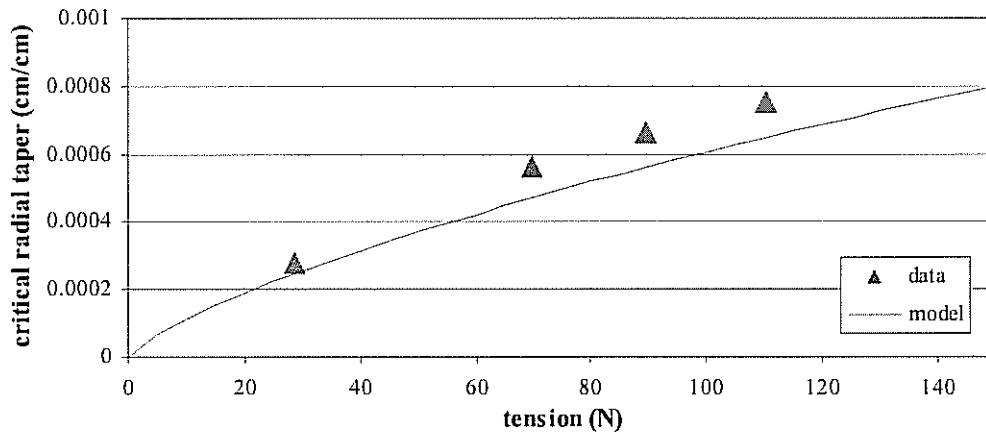


Figure 14 – 23.4 μm Polyester, $a = 50.8$ cm

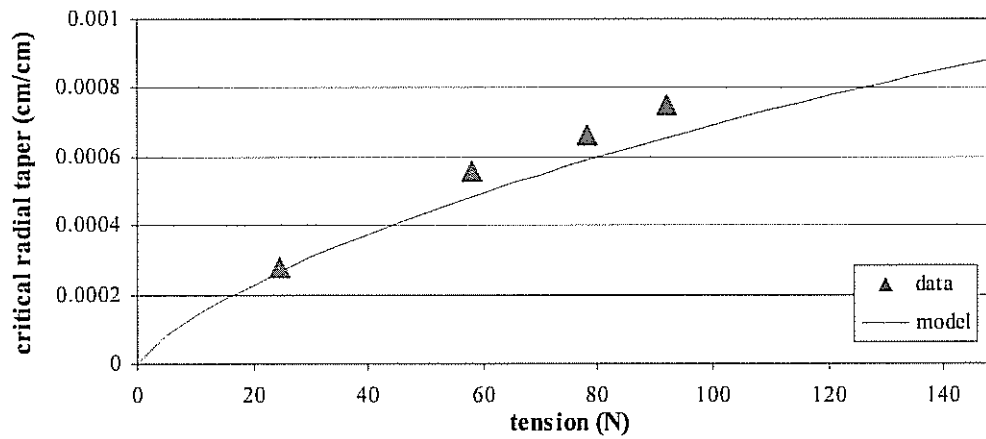


Figure 15 – 23.4 μm Polyester, $a = 76.2$ cm

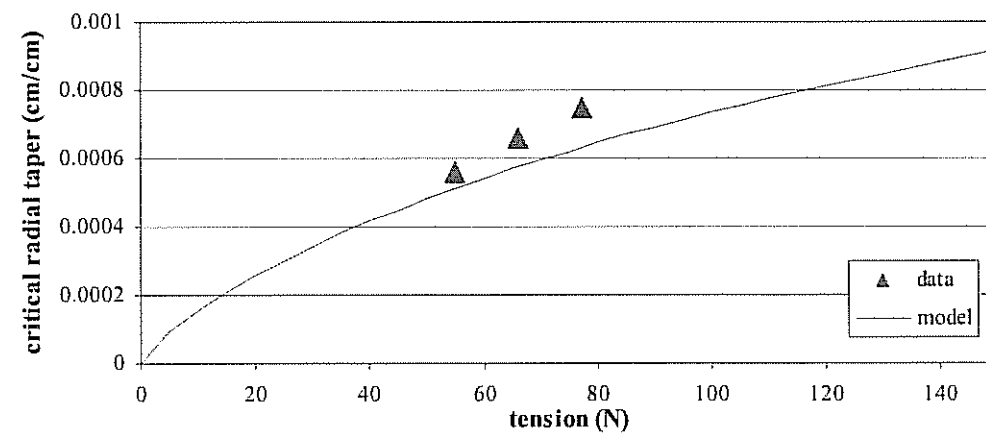


Figure 16 – 23.4 μm Polyester, $a = 101.6$ cm

The previous plots (Figures 13-16) each show the data recorded and a curve which shows where instability was predicted using expression (14). The area below the line is a region where planar web behavior is predicted as a function of roller taper and web tension. The region above the curve is where troughed web behavior is expected. It can be seen in all cases that the formation of troughs is not observed until after this line is crossed. The data also seems to follow the expected curvature of the theoretical line.

The next material tested was also polyester. It has a measured Young's Modulus of 4.5 GPa with a thickness of 14.2 μm . This material was able to be tested over 3 span lengths with the same procedure as used before. The results are shown in Figures 17 – 19.

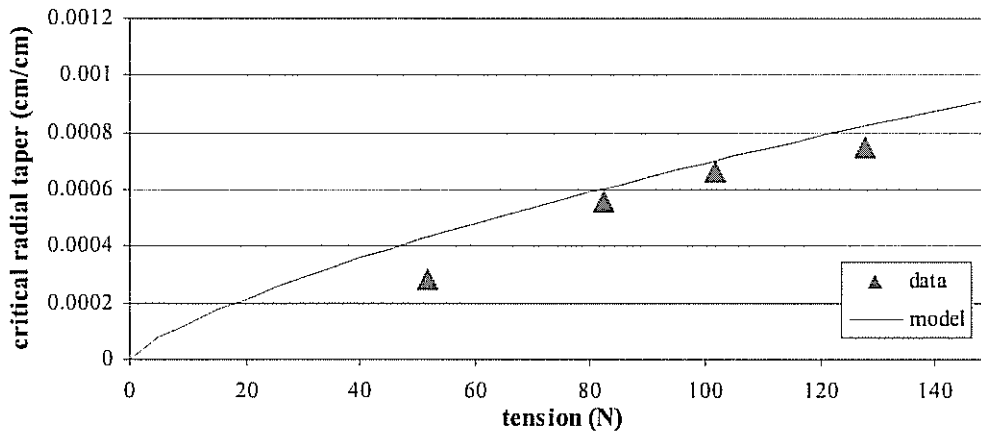


Figure 17 – 14.2 μm Polyester, $a = 50.8$ cm

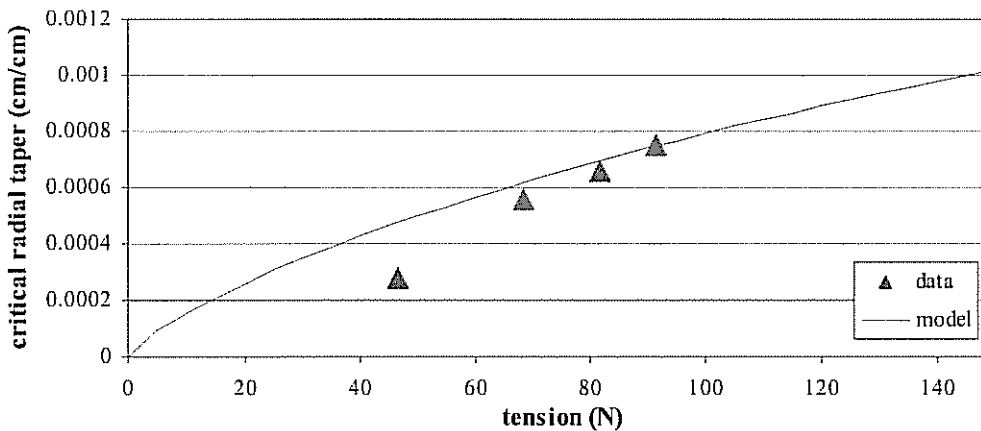


Figure 18 – 14.2 μm Polyester, $a = 76.2$ cm

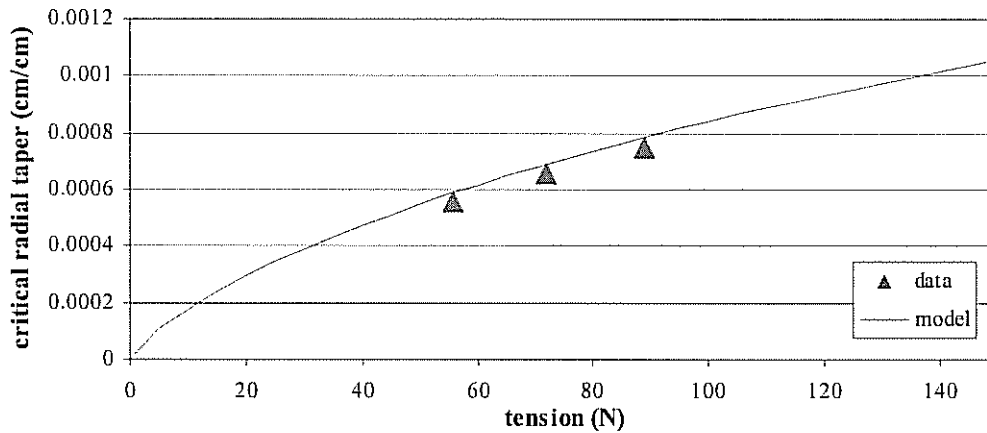


Figure 19 – 14.2 μm Polyester, $a = 101.2 \text{ cm}$

We can see that in the case of the 23.4 μm web, the troughs formed just below the line separating the troughed – planar region. One reason for this could be that caliper variation or other web non-uniformities are more critical to web stability in thinner webs. A slight web non-uniformity could cause a local stress increase that could lead to premature instability in the web. The web tested was a clear polyester so no deflection data could be collected for this web with the sensors employed in this study.

CONCLUSIONS

A web span under the influence of a downstream tapered roller has been modeled as a beam. The model describes the stress in the web, the lateral steering of the web, and the critical combination of taper and tension that cause instability in a web span. Experiments were conducted to test the proposed model for deflection over multiple spans and tensions. Additionally, the onset of troughs in the web was observed over multiple spans and two thicknesses. The results were then plotted against the proposed model with acceptable agreement. One observed point of interest is the presence of troughs does not seem to effect the deflection of the web at the tapered roller. The model presents a guideline for setting limits for taper on a roller and for predicting the lateral error a tapered roller introduces into a web line.

REFERENCES

1. Good, J.K., "Shear in Multispan Web Systems," Proceedings of the Fourth International Conference on Web Handling, Web Handling Research Center, Stillwater, Oklahoma, June 1997.
2. Good, J.K., Beisel, J.A., "Buckling of Orthotropic Webs in Process Machinery," Proceedings of the Seventh International Conference on Web Handling, Web Handling Research Center, Stillwater, Oklahoma, June 2003.
3. Lekhnitskii, S.G., Anisotropic Plates, Gordon and Breach Science Publishers, 1968.
4. Przemieniecki, J.S., Theory of Matrix Structural Analysis, McGraw-Hill, 1968.

5. Reddy, J. N., An Introduction to the Finite Element Method, 3rd ed., McGraw-Hill, 2006.
6. Shelton, J.J., "Effects of Web Camber on Handling," Proceedings of the Fourth International Conference on Web Handling, Web Handling Research Center, Stillwater, Oklahoma, June 1997.
7. Shelton, J.J., "Lateral Control of a Web," Internal Report, Web Handling Research Center, Stillwater, Oklahoma, June 2000.
8. Swift, H.W., "Camber for Belt Pulleys," Proceedings-Institute of Mechanical Engineers, June 1932.
9. Timoshenko, S.P., Gere, J.M., Theory of Elastic Stability, McGraw-Hill, 1963.
10. Vanderbilt, M.D., Matrix Structural Analysis, Quantum Publishers, USA, 1974.

Name & Affiliation

Mike Muncey
Goodyear

Question

I was interested in your technique where you use the laser light to determine when the trough was present. Was that something that can be totally automated where you could have it as part of a monitoring system? Where you off to the side without human intervention?

Name & Affiliation

Joe Beisel
Oklahoma State University

Answer

Yes, you could automate this but there was no need in this case. I was first concerned with trough experiments for misaligned rolls where it was a tedious process to visually detect the onset of troughs.

Name & Affiliation

Mike Muncy
Goodyear

Question

Have you seen this measurement made in part of a web process line for monitoring how well they are handling the web or to quantify the web quality?

Name & Affiliation

Joe Beisel
Oklahoma State University

Answer

No.

Name & Affiliation

Tim Walker
TJ Walker & Assoc.

Question

The curves you present look very similar to some of the shear wrinkle curves. You are plotting critical radius taper versus tension and observing when troughs form. You also plot lateral deflection of the web versus tension and observe when troughs form. This is very similar to the previous work where you studied how roller misalignment and web tension affect when troughs form. Have you mapped the web deflections due to tapered rollers which induce troughs versus the deflections from misaligned rollers which induce troughs? Would the deflections which induce troughs be similar for the two cases?

Name & Affiliation

Joe Beisel
Oklahoma State University

Answer

The fundamental shape of the web is considerably different when comparing the case of a web approaching a misaligned roll versus a web approaching a tapered roll. I would not expect the lateral deflection associated with the onset of troughs to be similar for the two cases.

Name & Affiliation

David Pfeiffer
JDP Innovations Inc.

Question

You introduced only one elastic modulus in your formulas and thus are assuming isotropic web properties. You used polyester in your trials, is it isotropic?

Name & Affiliation

Joe Beisel
Oklahoma State University

Answer

Both the stiffness matrix and the buckling criteria have already been extended to include orthotropic properties. In answer to your question we tested the modulus of this polyester web in both the machine and cross machine direction and found it to be isotropic.